Antineoplastic Agents. 529. Isolation and Structure of Nootkastatins 1 and 2 from the Alaskan Yellow Cedar *Chamaecyparis nootkatensis*†

George R. Pettit,* Rui Tan, Julian S. Northen, Delbert L. Herald, Jean-Charles Chapuis, and Robin K. Pettit

Cancer Research Institute and Department of Chemistry and Biochemistry, Arizona State University, Tempe, Arizona 85287-2404

Received September 16, 2003

The yellow cedar tree, *Chamaecyparis nootkatensis*, collected in southeast Alaska was evaluated as a potential source of new anticancer agents. Two new diterpene anticancer constituents termed nootkastatins 1 (**4**) and 2 (**5**) were isolated along with three previously known diterpene cancer cell growth inhibitors where two were reported as synthetic modifications of totarol and not previously found in nature. All five diterpene structures were established by HRMS and 1D and 2D NMR spectroscopic analyses combined with three X-ray crystal structure determinations (**2**, **3**, and **5**). Against a panel of six human cancer cell lines, this series of diterpenes exhibited inhibition over the range GI_{50} 0.75−2.0 μg/mL, and all inhibited the growth of Gram-positive bacteria and fungi.

The indigenous coastal people of British Columbia and southeast Alaska have a long history of utilizing the very tall (50 m) and long-lived (1−1.5 millennia commonly) yellow cedar tree, *Chamaecyparis nootkatensis* (Cupressaceae), for a variety of survival purposes ranging from bows to paddles and for medicinal purposes ranging from kidney ailments to mental illness to rheumatism.[2] The traditional medical uses of the yellow cedar, especially for kidney diseases, suggested that it should be investigated for potential anticancer and/or antimicrobial constituents. As a result, in August of 1998, we collected *C. nootkatensis* in the Tongass National Forest of southeast Alaska on Mitkof Island. Dichloromethane−methanol extracts of both the branches/leaves and bark/stemwood gave evidence of cancer cell growth inhibition against the P388 murine lymphocytic leukemia cell line and six human cancer cell lines.

Interestingly, while the investigation of *C. nootkatensis* has been ongoing for some fifty years, beginning with the pioneering research of Erdtman[3a−c] and others,[4a−d] the search for constituents with medicinal potential has only seriously begun in the past two years. Those studies have focused on antimicrobial activity[5] and the potentially important observation that the diterpene (+)-totarol from *C. nootkatensis* is active against *Mycobacterium tuberculosis*.[6] Another recent, potentially useful observation concerns the ability of *C. nootkatensis* to cause 100% mortality of the Formosan subterranean termite *Coptotermes formosanus* Shiraki.[7] The yellow cedar was one of only eight from a number of tree species that provided that level of protection. By employing bioassay-guided separation against the P388 murine lymphocytic leukemia and, for more advanced phases of the separations, a minipanel of human cancer cell lines, we have isolated five cancer cell line inhibitory diterpenes related to totarol where three (**1**−**3**) have been previously reported, and the two new ones are now designated nootkastatins 1 (**4**) and 2 (**5**). Each of the diterpenes exhibited antibacterial and antifungal activities. The summary of the isolation and structural elucidations now follows.

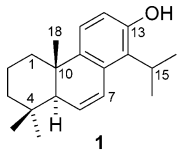

1

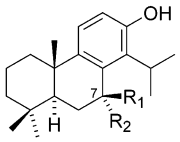

2, R_1 = H, R_2 = OH
3, R_1 = H, R_2 = OCH_3
4, R_1 = OCH_3, R_2 = H, nootkastatin 1

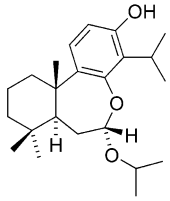

5, nootkastatin 2

The branches/leaves and stemwood/bark of *C. nootkatensis* were extracted separately with 1:1 dichloromethane−methanol, and the dichloromethane fractions were separately partitioned between methanol−water (9:1 → 3:2) and hexane−dichloromethane. The resulting dichloromethane fractions proved to be the best source of P388 leukemia cell line inhibitory constituents. The fractions were even more active against human cancer cell lines (Table 6). Consequently, the more advanced separations were guided by human cancer cell line results, and that was more necessary with the stemwood/bark origin fractions. The separations proceeded with an initial gel permeation chromatography in methanol on Sephadex LH-20. That was followed by a series of partition chromatographic steps on Sephadex LH-20 utilizing dichloromethane−methanol (3:2), hexane−2-propanol−methanol (8:1:1), toluene−dichloromethane−methanol (3:1:1), and hexane−toluene−methanol (3:1:1). The ultimate separations were performed using reverse-phase high-performance liquid chromatography followed by crystallization to afford diterpenes **1**−**3** and nootkastatins 1 (**4**) and 2 (**5**) in amounts ranging from 1.4 mg (**5**) to 24 mg (**3**) from 1.62 kg of stemwood/bark.

The yellow amorphous solid (**1**, 8.5 mg) was assigned structure **1**, a phenolic diterpene of the totarol type, on the basis of extensive mass and NMR (Table 1, ^{1}H and ^{13}C using ^{1}H−^{1}H COSY, and TOCSY, APT, and HMQC) spectroscopic interpretations. While this was the first isolation of abietane[8] **1**, it was reported in 1969 by Cambie

† Dedicated to the memory of Dr. Harry B. Wood (1919−2002), a U.S. National Cancer Institute pioneer in anticancer drug development.

* To whom correspondence should be addressed. Tel: 480-965-3351. Fax: 480-965-8558. E-mail: bpettit@asu.edu.

10.1021/np0304161 CCC: $27.50
Published on Web 07/22/2004

Table 1. ^{1}H and ^{13}C NMR Assignments for Phenol **1** (in $CDCl_3$, *J* in Hz)[a]

position	δ ^{1}H	^{1}H−^{1}H COSY	δ ^{13}C	HMBC (C to H)
1-CH_2	2.12 (1H, m, 1β)	H-1α, H-2α, β	36.67	H-2α, H-3β, H-18
	1.58 (1H, m, 1α)	H-1β		
2-CH_2	1.75 (1H, m, 2β)	H-1β, H-2α, H-3α, β	19.11	H-1α, β, H-3α
	1.68 (1H, m, 2α)	H-1β, H-2β, H-3α, β		
3-CH_2	1.53 (1H, m, 3β)	H-2α, β, H-3α	41.01	H-1β, H-2α, β, H-19, H-20
	1.20 (1H, m, 3α)	H-2α, β, H-3β		
4-C			32.64	H-2α, H-3α, β, H-5, H-6, H-19, H-20
5-CH	2.05 (1H, br, t, *J* = 3)	H-6, H-7	50.14	H-1β, H-3β, H-6, H-7, H-19, H-20
6-CH	6.05 (1H, dd, *J* = 10, 3)	H-5, H-7	130.84	H-5
7-CH	6.88 (1H, dd, *J* = 9.5, 3)	H-5, H-6	124.22	H-5
8-C			131.75	H-6, H-7, H-11, H-15
9-C			142.02	H-1α, β, H-7, H-11, H-12, H-18
10-C			38.31	H-1α, β, H-2α, H-5, H-6, H-11, H-18
11-CH	6.90 (1H, d, *J* = 8.5)	H-12	120.39	
12-CH	6.56 (1H, d, *J* = 8)	H-11	114.92	
13-C-OH	4.53 (1H, s, br)		152.24	H-11, H-12, H-15
14-C			129.50	H-7, H-12, H-15, H-16, H-17
15-CH	3.47 (1H, sept, *J* = 7)	H-16, H-17	27.40	H-16, H-17
16-CH_3	1.37 (3H, d, *J* = 6.5)	H-15	21.00	H-15, H-17
17-CH_3	1.39 (3H, d, *J* = 7.5)	H-15	21.28	H-15, H-16
18-CH_3	1.02 (3H, s)		20.31	H-1α, H-5
19-CH_3	1.05 (3H, s)		22.36	H-3α, H-5, H-20
20-CH_3	0.97 (3H, s)		32.55	H-3α, H-5, H-19

[a] ^{1}H and ^{13}C NMR were measured at 500 and 100 MHz, respectively.

Table 2. ^{1}H and ^{13}C NMR Assignments for Phenol **2** (in $CDCl_3$, *J* in Hz)

position	δ ^{1}H	^{1}H−^{1}H COSY	δ ^{13}C	HMBC (C to H)
1-CH_2	2.21 (1H, d, br, *J* = 15, 1β)	H-1α	39.09	H-3β, H-18
	1.33 (1H, m, 1α)	H-1β		
2-CH_2	1.59 (1H, m, 2β)	H-2α	19.46	H-1α, H-3α
	1.72 (1H, m, 1α)	H-2β, H-1β		
3-CH_2	1.48 (1H, m, 3β)	H-3α	41.37	H-1β, H-19, H-20
	1.25 (1H, m, 3α)	H-3β		
4-C			32.81	H-3α, H-5, H-6α, H-19, H-20
5-CH	1.60 (1H, dd, *J* = 16, 2)	H-6β	44.11	H-3β, H-6α,β, H-18, H-19, H-20
6-CH_2	1.89 (1H, dt, *J* = 5, 17, 6β)	H-5, H-6α, H-7	29.08	H-5
	1.99 (1H, d, br, *J* = 17, 6α)	H-6β		
7-CH	4.99 (1H, s, br)	H-6β	65.64	H-5, H-6α
8-C			134.59	H-6α, H-11, H-15
9-C			142.89	H-5, H-12, H-18
10-C			38.35	H-5, H-6α,β, H-11, H-18
11-CH	7.00 (1H, d, *J* = 8.4)	H-12	123.46	
12-CH	6.60 (1H, d, *J* = 8.8)	H-11	117.06	H-13
13-C-OH	4.51 (1H, s)		152.81	H-11, H-12, H-13, H-15
14-C			133.02	H-12, H-13, H-15, H-16, H-17
15-CH	3.55 (1H, sept, *J* = 8.5)	H-16, H-17	27.60	H-16, H-17
16-CH_3	1.40 (3H, d, *J* = 6.8)	H-15	20.93	H-15, H-17
17-CH_3	1.36 (3H, d, *J* = 7.2)	H-15	21.67	H-15, H-16
18-CH_3	1.11 (3H, s)		24.49	H-1β, H-5
19-CH_3	0.96 (3H, s)		33.05	H-3α, H-5, H-20
20-CH_3	0.90 (3H, s)		21.67	H-3α, H-5, H-19

as a synthetic intermediate.[9] Extension of the analogous detailed mass and NMR spectral interpretations to diterpenes **2** and **3** as summarized in the Experimental Section and Tables 2 and 3 led to the assignment of structures **2** and **3** with the stereochemistry at C-7 in doubt. Fortunately, both phenols **2** and **3** crystallized nicely from methanol. These X-ray-quality crystals allowed crystal structure determinations of both phenols **2** and **3** and establishment of the stereochemistry at C-7 as shown. Those results clearly established the C-7 hydroxy and methoxy substituents of diterpenes **2** and **3** as alpha. The X-ray crystal structures (see Figures 1 and 2) also provided an explanation for the H-7 proton NMR signal appearing as a broad singlet. The A/B rings were found to be in a chair and half-chair conformation owing to the 7α-substituents in axial positions.

Diterpene **2** had also not previously been isolated from a natural source and was reported as a synthetic intermediate in 1962,[10] providing a second example in the present study of those rare instances where an anticancer natural product had been earlier described as a synthetic objective.[11] After we had arrived at the structure of methyl ether **3**, it was reported to arise from the ethyl acetate extract of the resinous stem canker of *T. dolobrata* var. *hondae*.[12]

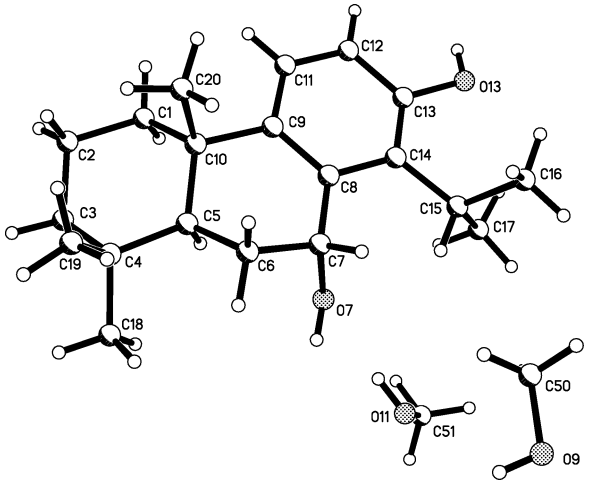

Figure 1. X-ray structure of phenol **2**. The two solvent molecules of methanol are also shown.

Table 3. ^{1}H and ^{13}C NMR Assignments for Phenol **3** (in $CDCl_3$, *J* in Hz)

position	δ ^{1}H	^{1}H−^{1}H COSY	δ ^{13}C	HMBC (C to H)
1-CH_2	2.17 (1H, d, br, *J* = 13, 1*β*)	H-1α	38.97	H-2α, H-3α,*β*, H-5, H-18
	1.40 (1H, m, 1α)	H-1*β*, H-2α,*β*		
2-CH_2	1.57 (1H, m, 2*β*)	H-1α, H-2α, H-3α,*β*	19.47	H-1α,*β*, H-3α,*β*
	1.72 (1H, m, 2α)	H-1α, H-2*β*, H-3α,*β*		
3-CH_2	1.46 (1H, d, br, *J* = 13, 3*β*)	H-2α,*β*, H-3α	41.14	H-1α,*β*, H-2*β*, H-5, H-19, H-20
	1.24 (1H, dt, *J* = 4, 13, 3α)	H-2α,*β*, H-3*β*		
4-C			32.86	H-2*β*, H-3α,*β*, H-6α, H-5, H-19, H-20
5-CH	1.69 (1H, d, br, *J* = 13)	H-6α,*β*	43.80	H-1*β*, H-3*β*, H-6α,*β*, H-18, H-19, H-20
6-CH_2	1.60 (1H, m, 6*β*)	H-5, H-6α, H-7	22.19	H-5
	2.20 (1H, d, br, *J* = 14, 6α)	H-5, H-6*β*, H-7		
7-CH	4.39 (1H, s, br)	H-6α,*β*	74.74	H-5, H-6α, H-21
8-C			133.21	H-6α, H-7, H-11, H-15
9-C			143.06	H-1α, H-5, H-7, H-12, H-18
10-C			38.23	H-1α, H-5, H-6α,*β*, H-11, H-18
11-CH	6.98 (1H, d, *J* = 6.4)	H-12	123.30	
12-CH	6.58 (1H, d, *J* = 7.2)	H-11	117.10	H-13
13-C-OH	4.56 (1H, s)		152.50	H-11, H-12, H-13, H-15
14-C			133.27	H-12, H-15, H-16, H-17
15-CH	3.11 (1H, sept, *J* = 6)	H-16, H-17	27.86	H-16, H-17
16-CH_3	1.40 (3H, d, *J* = 7)	H-15	20.40	H-15, H-17
17-CH_3	1.38 (3H, d, *J* = 7)	H-15	20.85	H-15, H-16
18-CH_3	1.12 (3H, s)		24.43	H-1α,*β*, H-5
19-CH_3	0.97 (3H, s)		32.93	H-3α,*β*, H-5, H-20
20-CH_3	0.92 (3H, s)		21.71	H-3α,*β*, H-5, H-19
21-CH_3	3.41 (3H, s)		55.18	H-7

Table 4. ^{1}H and ^{13}C NMR Assignments for Nootkastatin 1 (**4**) (in $CDCl_3$, *J* in Hz)

position	δ ^{1}H	^{1}H−^{1}H COSY	δ ^{13}C	HMBC (C to H)
1-CH_2	2.18 (1H, d, br, *J* = 12, 1*β*)	H-1α, H-2α,*β*	40.03	H-18
	1.26 (1H, m, 1α)	H-1*β*		
2-CH_2	1.65 (1H, m, 2*β*)	H-1*β*, H-2α, H-3α,*β*	19.45	H-1*β*
	1.71 (1H, m, 2α)	H-1*β*, H-2*β*, H-3α,*β*		
3-CH_2	1.44 (1H, m, 3*β*)	H-2α, *β*, H-3α	41.78	H-1*β*, H-19, H-20
	1.18 (1H, m, 3α)	H-2α, *β*, H-3*β*		
4-C			33.39	H-3α, H-19, H-20
5-CH	1.23 (1H, m)	H-6α	48.54	H-1*β*, H-6α,*β*, H-18, H-19, H-20
6-CH_2	1.75 (H, dt, *J* = 13.5, 8, 6*β*)	H-6α, H-7	25.84	H-7
	2.36 (1H, ddd, *J* = 13, 9, 2.4, 6α)	H-5, H-6*β*, H-7		
7-CH	4.66 (1H, t, *J* = 8.4)	H-6α,*β*	76.15	H-5, H-6α,*β*, H-21
8-C			134.35	H-6α, H-7, H-11, H-15
9-C			144.94	H-7, H-11, H-18
10-C			37.86	H-6α,*β*, H-11, H-18
11-CH	6.93 (1H, d, *J* = 8.8)	H-12	122.55	
12-CH	6.55 (1H, d, *J* = 8.4)	H-11	116.64	
13-C-OH	4.51 (1H, s, br)		152.94	H-11, H-12, H-15
14-C			133.79	H-12, H-15, H-16, H-17
15-CH	3.14 (1H, sept, *J* = 7.6)	H-16, H-17	28.77	H-16, H-17
16-CH_3	1.40 (3H, d, *J* = 7)	H-15	20.85	H-15, H-17
17-CH_3	1.32 (3H, d, *J* = 7.6)	H-15	21.20	H-15, H-16
18-CH_3	1.23 (3H, s)		24.64	H-5
19-CH_3	0.92 (3H, s)		33.13	H-20
20-CH_3	0.93 (3H, s)		21.67	H-19
21-CH_3	3.41 (3H, s)		54.55	H-7

The HRFABMS data for nootkastatin 1 (**4**, 3.6 mg) led to the molecular formula $C_{21}H_{32}O_2$, isomeric with that of diterpene **3**. Interpretation of the NMR spectroscopic results (Table 4) established the same abietane skeleton as that represented by phenol **3**. However, the chemical shifts apparent at C-5, C-6, and C-7, combined with a doublet signal splitting for 7-H shown by nootkastatin 1 (**4**) versus a broad signal for phenol **3**, readily allowed the conclusion that phenol **3** and nootkastatin 1 (**4**) were epimeric at C-7. Therefore, nootkastatin 1 (**4**) was the 7*β*-methoxy epimer of the known 7α-methoxytotarol (**3**).[12] A referee thoughtfully suggested that since the 7-OH in diterpene **2** is at a benzylic position, it could have undergone solvolysis to give methyl ethers **3** and **4**. However, we found that when a methanol solution of alcohol **2** was retained at room temperature for several days, the residue after removal of solvent was shown by NMR analysis to consist only of alcohol **2**. Therefore, methyl ethers **3** and **4** are not likely to be solvolysis artifacts.

The molecular formula of nootkastatin 2 (**5**), based on HRMS, proved to be $C_{23}H_{36}O_3$ in detailed NMR analyses (Table 5), indicating the presence of an additional isopropyl group in place of the methyl group at C-7 of nootkastatin 1. Information from the HMBC experiments suggested that C-7 and C-8 were now bonded through an oxygen atom, pointing to an acetal unit emanating from C-7 and including the second isopropyl group, leading to this abietane B-ring as a seven-membered oxygen heterocycle. Those assumptions and unequivocal evidence for the overall structure and configuration were established by X-ray crystal structure determination (Figure 3).

Trees of the *Podocarpus* (Podocarpaceae), as well as the taxodiaceae,[8d] have in the past proven to be useful sources

Table 5. ^{1}H and ^{13}C NMR Assignment for Nootkastatin 2 (**5**) (in $CDCl_3$, *J* in Hz)

position	δ ^{1}H	^{1}H-^{1}H COSY	δ ^{13}C	HMBC (C to H)
1-CH_2	2.11 (1H, m, 1*β*)	H-1α, H-2α,*β*	44.25	H-3α
	1.28 (1H, m, 1α)	H-1*β*		
2-CH_2	1.46 (1H, m, 2*β*)	H-1*β*, H-2α, H-3α,*β*	19.62	H-1*β*
	1.60 (1H, m, 2α)	H-1*β*, H-2*β*, H-3α,*β*		
3-CH_2	1.36 (1H, m, 2*β*)	H-2α,*β*, H-3α	42.16	H-19
	1.20 (1H, m, 2α)	H-2α,*β*, H-3*β*		
4-C			33.99	H-2*β*, H-3α, H-5, H-6α,*β*, H-19, H-20
5-CH	2.02 (1H, m)	H-6α	45.38	H-1α, H-3α,*β*, H-6α,*β*, H-18, H-19, H-20
6-CH_2	2.02 (1H, m, 6*β*)	H-6α, H-7	34.32	H-7
	2.20 (1H, m, 6α)	H-5, H-6*β*, H-7		
7-CH	4.88 (1H, dd, *J* = 7, 3)	H-6α,*β*	103.87	H-5, H-6α,*β*, H-21
8-C			153.22	H-7, H-11, H-15
9-C			135.65	H-5, H-11, H-18
10-C			41.48	H-5, H-6α,*β*, H-11, H-18
11-CH	7.02 (1H, d, *J* = 7.2)	H-12	126.5	
12-CH	6.38 (1H, d, *J* = 7.2)	H-12	111.04	H-13
13-C-OH	4.55 (1H, s)		152.65	H-11, H-12, H-13
14-C			124.18	H-12, H-13, H-15, H-16, H-17
15-CH	3.80 (1H, sept, *J* = 7)	H-16, H-17	24.26	H-16, H-17
16-CH_3	1.35 (3H, d, *J* = 7.5)	H-15	21.03	H-15
17-CH_3	1.34 (3H, d, *J* = 7.0)	H-15	20.36	H-15
18-CH_3	1.38 (3H, s)		24.72	H-5
19-CH_3	1.00 (3H, s)		33.58	H-3α,*β*, H-20
20-CH_3	0.97 (3H, s)		23.34	H-5, H-20
21-CH	3.92 (1H, sept, *J* = 6)	H-22, H-23	70.01	H-7, H-22, H-23
22-CH_3	1.29 (3H, d, *J* = 6)	H-21	23.26	H-21, H-23
23-CH_3	1.10 (3H, d, *J* = 6)	H-21	21.59	H-22

Table 6. Inhibition Values of Murine P388 Lymphocytic Leukemia Cell Line[a] (ED_{50} in *μ*g/mL) and Human Cancer Cell Line (GI_{50} in *μ*g/mL) for Compounds **1**−**5**

cancer cell line[b]	**1**	**2**	**3**	**4**	**5**
P388	3.7	1.7	>10	1.5	5.8
BXPC-3	>10	1.8	1.5	2.1	1.8
MCF-7	>10	2.1	1.5	2.0	2.3
SF268	>10	2.3	1.9	0.85	2.0
NCI-H460	>10	1.8	1.8	0.75	2.0
KM20L2	>10	2.3	1.6	0.98	2.4
DU-145	>10	2.6	1.7	1.1	2.2

[a] In DMSO. [b] Human cancer type: BXPC-3 (pancreas adenocarcinoma); MCF-7 (breast adenocarcinoma); SF268 (CNS glioblastoma); NCI-H460 (lung large cell); KM20L2 (colon adenocarcinoma); DU-145 (prostate carcinoma).

of totarol and related diterpenes.[8a−d] As summarized in Table 6, an evaluation of diterpenes **1**−**5** against the P388 lymphocytic leukemia and six human cancer cell lines revealed nootkastatin 1 (**4**) to be the most significant cancer cell growth inhibitor. Occasionally, related diterpenes have been found to have cancer cell growth inhibitory activities.[13a,b]

The antibacterial activity of totarol was first reported in 1992.[14] Since that time, there have been numerous publications concerning the antimicrobial properties of totarol, synthetic derivatives of totarol, and related diterpenes.[15−22] Totarol is active against Gram-positive bacteria[14−16,18] and acid-fast bacteria (*Mycobacterium* spp.),[16] and its mechanism of action involves perturbation of membrane structure.[21,22] In the present study, the antimicrobial spectrum of diterpenes **1**−**5** was evaluated. All five compounds were active against Gram-positive bacteria and the pathogenic yeast *Cryptococcus neoformans* (Table 7). The only Gram-negative organism inhibited was *Neisseria gonorrhoeae* (Table 7). The susceptibility of *N. gonorrhoeae* to antibiotics bears more resemblance to Gram-positive than Gram-negative bacteria, due to short chain lipopolysaccharides in the outer membrane. Only phenol **2** had activity (marginal) against the opportunistic yeast *Candida albicans* (Table 7). To determine if nootkastatins 1 and 2 were bactericidal or bacteristatic, minimum bactericidal concentrations (MBCs) were determined. In most cases, MBCs were no more than two, 2-fold dilutions

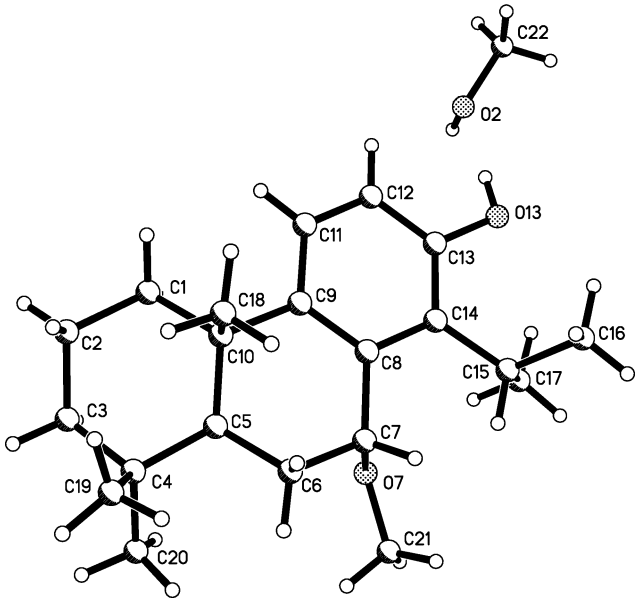

Figure 2. X-ray structure of phenol **3**. The solvent molecule methanol is also shown.

higher than minimum inhibitory concentrations (MICs) (Table 7), suggesting a cidal mechanism of action.

Overall, phenol **3** had the lowest MICs, and thus its activity against antibiotic-resistant clinical isolates was investigated. The MICs for antibiotic-resistant strains (Table 8) were similar to those obtained with the reference strains (Table 7). As indicated by MFC (minimum fungicidal concentration)/MIC and MBC/MIC ratios, phenol **3** was also cidal for the antibiotic-resistant strains (Table 8). Although the isolation of **3** from *Thujopsis dolabrata* var. *hondae* was published in 2002,[12] this is the first report of microbial and cancer cell line growth inhibition. Compounds **3**−**5** were available in sufficient quantity to investigate the effect of human serum on MICs. MICs in 25% human serum were >64 *μ*g/mL for all strains tested (2−3 strains/compound, data not shown), suggesting that this group of compounds should be pursued as topical and not systemic agents of antimicrobial therapy.

Table 7. Antimicrobial Activities of Diterpenes **1**−**5**

microorganism	ATCC (or Presque Isle) #	MIC (μg/mL)/MBC[b] (μg/mL) compound **1**	**2**	**3**	**4**	**5**
Cryptococcus neoformans	90112	16	16	8	64	64
Candida albicans	90028	*a*	64	*a*	*a*	*a*
Staphylococcus aureus	29213	16	16	4	8/32	4/8
Streptococcus pneumoniae	6303	32	16	8	64/64	64/64
Enterococcus faecalis	29212	16	16	4	4/16	2/32
Micrococcus luteus	(456)	4	8	2	2/8	1/16
Escherichia coli	25922	*a*	*a*	*a*	*a*	*a*
Enterobacter cloacae	13047	*a*	*a*	*a*	*a*	*a*
Stenotrophomonas maltophilia	13637	*a*	*a*	*a*	*a*	*a*
Neisseria gonorrhoeae	49226	8	8	4	2/4	2/2

[a] No inhibition at 64 μg/mL. [b] Only determined for **4** and **5**.

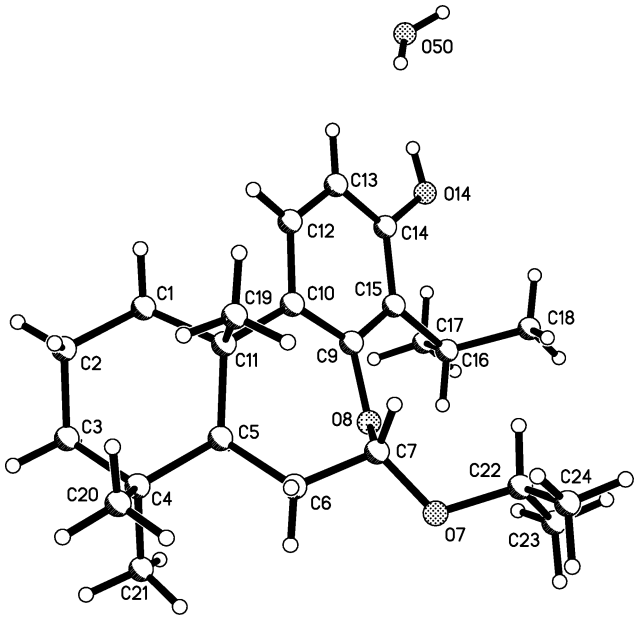

Figure 3. X-ray structure of nootkastatin 2 (**5**). The solvent water is also shown.

Table 8. Expanded Antimicrobial Evaluation of Diterpene **3**

clinical isolate or (reference strain)	MIC (μg/mL)/ MFC or MBC (μg/mL)
fluconazole-resistant *Cryptococcus neoformans*	4/4
Candida glabrata	*a*
methicillin-resistant *Staphylococcus aureus*	4/8
Staphylococcus epidermidis (ATCC 49461)	2/16
penicillin-resistant *Streptococcus pneumoniae*	16/16
penicillin-resistant *Streptococcus pyogenes*	16/32
vancomycin-resistant *Enterococcus faecium*	4/4
Rhodococcus spp.	2/8

[a] No inhibition at 64 μg/mL.

In summary, the Haida, Kwakwaka'wakw, and Salish certainly had some basis for certain medicinal application of teas prepared from *C. nootkatensis*, one of the most magnificent and useful trees.[2] Indeed, this has not gone unnoticed by a broad audience, and one observer has recorded, "O, the cedar tree! If mankind in his infancy had prayed for the perfect substance for all materials and aesthetic needs, an indulgent God could have provided nothing better."[23]

Experimental Section

General Experimental Procedures. Solvents used for chromatographic procedures were redistilled. The Sephadex LH-20 employed for gel permeation and partition chromatography was obtained from Pharmacia Fine Chemicals AB, Uppsala, Sweden. The silica gel GHLF Uniplates for thin-layer chromatography were supplied by Analtech, Inc. The TLC results were viewed under UV light and developed with $Ce(SO_4)_2-H_2SO_4$ (heating for 3 min). Reverse-phase HPLC experiments were performed on Luna C8 (250 × 10 mm, 5 μm), Zorbax SB C18 (250 × 4.6 mm, 5 μm), and Discovery C8 (250 × 4.6 mm, 5 μm) columns with either Gilson HPLC or Hewlett-Packard 1100 series instruments monitored with UV and ELSD detectors. Optical rotation data were determined with a Perkin-Elmer 241 polarimeter. Ultraviolet spectra were observed using a Perkin-Elmer Lambda 3β UV/vis spectrophotometer equipped with a Hewlett-Packard laser jet 2000 plotter. IR spectra were recorded using an Avatar 360 FT-IR instrument with the sample prepared in a $CHCl_3$ film. High-resolution mass spectra were obtained using a JEOL mass spectrometer. The NMR experiments were conducted using a Varian Unity Inova 500 spectrometer operating at 500 and 100 MHz for ^1H and ^{13}C NMR, respectively.

Yellow Cedar Collection. In August 1998 in the Tongass National Forest on Mitkof Island in southeast Alaska, the branches/leaves (12.7 kg) and stemwood/bark (1.62 kg) of *C. nootkatensis* (D. Don) Spach were collected. In the few days preceding collection, this several hundred year old and very healthy appearing tree had been felled for apparent logging purposes. The fresh (wet) tree parts were shipped to our Institute, and extraction began soon after arrival. Along the Coastal Pacific Northwest, this yellow cedar is also known as yellow cypress and Alaska cedar.[2] The leaves of yellow cedar are similar to those of western red cedar, but when crushed, the yellow cedar leaves have "an unpleasant, mildew smell"[2] in contrast to the pleasing odor emitted by red cedar foliage.[2]

Extraction and Initial Separation of *C. nootkatensis*. The branches/leaves (12.7 kg) of the yellow cedar were extracted twice with 1:1 $CH_2Cl_2-CH_3OH$. After each extraction, 30% H_2O by volume was added to separate the CH_2Cl_2 phase. The solvent was removed (in vacuo) from the first CH_2Cl_2 fraction (726 g, P388 ED_{50} 20 μg/mL, HCL GI_{50} 3−8 μg/mL) and from the second CH_2Cl_2 fraction (278 g, P388 ED_{50} 27 μg/mL, HCL GI_{50} 10−13 μg/mL). The CH_3OH-H_2O fractions from the initial extraction steps were essentially inactive against both sets of cancer cell lines. A 1 kg aliquot of the combined (black tar appearance) CH_2Cl_2 fractions was dissolved with stirring in 4.8 L of hexane. The hexane solution was extracted (4×) with 4.8 L of 9:1 CH_3OH-H_2O to yield a CH_3OH-H_2O fraction, which was then diluted to 3:2 CH_3OH-H_2O by the addition of 2.4 L of H_2O. The solvent partitioning sequence then continued with CH_2Cl_2 (total of 5 L, 3×) based on our modification of the early Bligh and Dyer procedure.[24] The resulting cancer cell line active CH_2Cl_2 fraction (236.8 g) was then employed in the subsequent separation procedures.

The preceding solvent partitioning sequence using the CH_2Cl_2 fractions from the branches/leaves provided 711.8, 236.8, and 53.8 g of hexane, CH_2Cl_2, and CH_3OH-H_2O fractions, respectively. The stemwood/bark (1.62 kg) was subjected to a similar solvent partitioning procedure. The yields were 41.8 g (hexane), 90.8 g (CH_2Cl_2), and 2.4 g (CH_3OH-H_2O).

Isolation. The active CH_2Cl_2 fraction (90.8 g) from the stemwood/bark was dissolved in CH_3OH, and the solution was filtered to remove 4.0 g of brown solid. Evaporation of solvent gave a 86.5 g residue that was used for an initial chromatography in CH_3OH on a 10 cm diameter Sephadex LH-20 column that produced 10 fractions. Two of the cancer cell inhibitory fractions were combined and further separated using Sephadex LH-20 column partition chromatography with the following series of solvent systems: $CH_2Cl_2-CH_3OH$ (3:2); hexane−2-propanol−CH_3OH (8:1:1); toluene−$CH_2Cl_2-CH_3OH$ (3:1:1); hexane−toluene−CH_3OH (3:1:1). The final stage of separation was performed using reverse-phase HPLC on a Zorbax SB C18 column with a CH_3CN-H_2O (40%−90%) gradient to yield (t_R 22 min) phenol **1**: yellowish amorphous solid (8.5 mg). HPLC of the next active fraction on a Discovery C8 column with the same solvent and gradient led to phenol **2** (t_R 17 min) as colorless needles (9.1 mg) from CH_3OH. A third active fraction was separated by HPLC on a Luna C8 column (5 μm) in $CH_3CN-CH_3OH-H_2O$ (50:35:15) to provide phenol **3** (t_R 55 min) as colorless crystals (21 mg) from CH_3OH. The other active fractions were combined and separated by reverse-phase HPLC on Zorbax SB C18 in $CH_3CN-CH_3OH-H_2O$ (50:25:25) to give two more concentrated active fractions, which were further separated using a Discovery C8 column with a gradient of the same solvent mixture to yield nootkastatin 1 (**4**, 3.6 mg) as an amorphous powder and nootkastatin 2 (**5**, 1.4 mg) as colorless crystals.

Characterization of Phenols 1−3 and Nootkastatins 1 and 2. Phenol 1: mp 75−78° C (lit.[9] as gum); $[\alpha]_D^{23}$ −25.0° (*c* 0.04, $CHCl_3$); UV ($CHCl_3$) λ_{max} (log ϵ) 240 nm (3.74); IR ($CHCl_3$) ν_{max} 3360, 2923, 1585, 1246, 1099, 629 cm^{-1}; HRFABMS *m/z* 285.2214 $[M + H]^+$, calcd for $C_{20}H_{29}O$, 285.2218; ^1H, ^{13}C NMR, $^1H,^1H$-COSY, and HMBC data (see Table 1).

Phenol 2: colorless needles from CH_3OH; mp 214−215 °C (lit.[10] mp 215−217° C); $[\alpha]_D^{23}$ +7.76° (*c* 0.58, $CHCl_3$); UV ($CHCl_3$) λ_{max} (log ϵ) 281 (3.32), 240 (3.32) nm; IR ($CHCl_3$) ν_{max} 3312, 2946, 1585, 1284, 1192, 1034, 815 cm^{-1}; HRFABMS *m/z* 285.2215 $[M + H - H_2O]^+$, calcd for $C_{20}H_{29}O$, 285.2218; ^1H NMR ($CDCl_3$, 500 MHz) and ^{13}C NMR ($CDCl_3$, 100 MHz), $^1H,^1H$-COSY, and HMBC (see Table 2).

X-ray Crystallographic Analysis of Phenol 2. Crystal data: $C_{20}H_{30}O_2 \cdot 2CH_3OH$, M_r = 366.52, monoclinic, $P2_1$, a = 7.542(2) Å b = 19.429(7) Å, c = 7.825(3) Å, β = 109.830(18)°, V = 1078.5(7) Å, Z = 2, ρ = 1.129 Mg/m^3, μ(Cu Kα) = 0.597 mm^{-1}, λ = 1.54178 Å, $F(000)$ = 404. Frames of reflections covering a complete sphere of reflections were collected on a colorless crystal (0.28 × 0.23 × 0.10 mm), equivalent to a θ range of 6.24−68.35° using φ and ω scans with the Bruker Multirun scan procedure. From these frames, a total of 6239 reflections were harvested using the narrow frame algorithm of the program SAINT-PLUS,[25] which also performed data reduction, merging of equivalent reflections, and decay corrections. A total of 3336 independent reflections (R_{int} = 0.1073) remained, of which 1779 reflections were considered observed ($I_o \geq 2\sigma(I_o)$) and were used in subsequent structure solution and refinement with SHELXTL.[26] All non-hydrogen atom coordinates of the parent molecule **2** were located in a routine run of SHELXS,[26] along with two molecules of CH_3OH solvent. The H atom coordinates for all molecules were calculated at optimum positions. All non-hydrogen atoms were refined anisotropically in a full-matrix least-squares process. The hydrogen atoms were included, and their U_{iso} thermal parameters were fixed at 1.2 or 1.5 (depending on atom type) times the values of the atom to which they were attached and forced to ride that atom. The final residual R_1 value obtained for the model of phenol **2**, which also contained two molecules of methanol (shown in Figure 1), was 0.1171 for the observed data and 0.1597 for all data. The goodness of fit was 1.115. Minimal electron density was exhibited in the final difference Fourier map with the largest peak of 0.357 e/Å^3 and hole of −0.373 e/Å^3. The Flack *x* parameter was −0.7059, with an esd of 0.9500, implying that the absolute configuration could not be determined reliably. Figure 1 represents one of the possible stereostructures, which would correspond to the related phenol **3**. The final bond distances and angles were all within expected and acceptable limits.

Phenol 3: colorless crystals from CH_3OH; mp 130−133 °C (lit.[12] as colorless oil); $[\alpha]_D^{23}$ +20.0° (*c* 0.30, $CHCl_3$); UV ($CHCl_3$) λ_{max} (log ϵ) 280 (3.38), 239 (2.94) nm; IR ($CHCl_3$) ν_{max} 3350, 2923, 1585, 1279, 1186, 1066, 815 cm^{-1}; HRFABMS *m/z* 285.2215 $[M + H - CH_3OH]^+$, calcd for $C_{20}H_{29}O$, 285.2218; ^1H NMR ($CDCl_3$, 500 MHz), ^{13}C NMR ($CDCl_3$, 100 MHz), $^1H,^1H$-COSY, and HMBC are summarized in Table 3.

X-ray Crystallographic Analysis of Phenol 3 (3). Crystal data: $C_{21}H_{32}O_2 \cdot 1CH_3OH$, M_r = 348.51, monoclinic, $P2_1$, a = 9.2700(1) Å, b = 9.9807(1) Å, c = 12.0636(2) Å, β = 107.0970(10)°, V = 1066.81(2) Å^3, Z = 2, ρ = 1.085 Mg/m^3, μ(Cu Kα) = 0.546 mm^{-1}, λ = 1.54178 Å, $F(000)$ = 384. In a manner analogous to that described for phenol **2**, data collection and refinement were conducted on a crystal of phenol **3** (0. 0.64 × 0.32 × 0.16 mm) at 123 K. A total of 7920 independent reflections (R_{int} = 0.0271) were collected, of which a total of 3236 were considered observed ($I_o \geq 2\sigma(I_o)$) and used in refinement. The final residual R_1 value for the model used for phenol 3 (**3**) with the methanol solvent in Figure 2 was 0.0478 for the observed data and 0.0498 for all data (3431 reflections). The goodness of fit was 1.078. Minimal electron density was exhibited in the final difference Fourier map with the largest peak of 0.298 e/Å^3 and hole of −0.234 e/Å^3. Refinement of the Flack *x* parameter for the structure shown in Figure 2, using the TWIN/BASF options in SHELXL, resulted in a value of 0.00001 with an esd of 0.21719. Refinement of the opposite enantiomeric form of **3** resulted in a Flack parameter of 1.0277 with an esd of 0.21727. Although these values would tend to indicate that the correct absolute configuration of phenol **3** is indeed that represented in Figure 2, the large esd (>0.1) precludes the assignment of absolute configuration with certainty (i.e., >99.99% confidence level), implying that the absolute configuration of the structure for phenol **3** is uncertain. The final bond distances and angles were all within expected and acceptable limits.

Nootkastatin 1 (4): colorless amorphous powder, mp 52−54 °C; $[\alpha]_D^{23}$ +14.0° (*c* 0.05, $CHCl_3$); UV ($CHCl_3$) λ_{max} (log ϵ) 281 (3.15), 240 (3.06) nm; IR ($CHCl_3$) ν_{max} 3368, 2926, 1459, 1279, 1113, 1076, 668 cm^{-1}; HRFABMS *m/z* 285.2218 $[M + H - CH_3OH]^+$ calcd for $C_{20}H_{29}O$, 285.2218; refer to Table 4 for its ^1H NMR ($CDCl_3$, 500 MHz), ^{13}C NMR ($CDCl_3$, 100 MHz), $^1H,^1H$-COSY, and HMBC.

Nootkastatin 2 (5): colorless crystals from CH_3OH, mp 87−88 °C, $[\alpha]_D^{23}$ +98.6° (0.07, $CHCl_3$); UV ($CHCl_3$) λ_{max} (log ϵ) 281 (3.12), 241 (3.37) nm; IR ($CHCl_3$) ν_{max} 3392, 2927, 1599, 1423, 1124, 1004, 668 cm^{-1}; HRFABMS *m/z* 361.2794 $[M + H]^+$ (calcd for $C_{23}H_{37}O_3$, 361.2743); ^1H NMR ($CDCl_3$, 500 MHz), ^{13}C NMR ($CDCl_3$, 100 MHz), $^1H,^1H$-COSY, and HMBC are summarized in Table 5.

X-ray Crystallographic Analysis of Nootkastatin 2 (**5**). Crystal data: $C_{23}H_{36}O_3 \cdot 1H_2O$, M_r = 378.53, trigonal, $P3_1$, a = 12.3902(4) Å, b = 12.3902(4) Å, c = 12.7629(7) Å, γ = 120.0°, V = 1696.82(12) Å^3, Z = 3, ρ = 1.111 Mg/m^3, μ(Cu Kα) = 0.585 mm^{-1}, λ = 1.54178 Å, $F(000)$ = 624. Data collection and refinement were conducted on a crystal of phenol **5** (0.32 × 0.26 × 0.16 mm) at 123 K. A total of 11 379 independent reflections were harvested. Data reduction and merging of equivalent reflections (R_{int} = 0.0806) resulted in a total of 3782 reflections, of which 2626 were considered observed ($I_o \geq 2\sigma(I_o)$) and used in refinement with SHELXTL.[26] The final residual R_1 value for the model shown in Figure 3 for nootkastatin 2 (**5**) with one molecule of water solvent was 0.0744 for the observed data and 0.0985 for all data (3782 reflections). The goodness of fit was 0.947. Minimal electron density was exhibited in the final difference Fourier map with the largest peak of 0.298 e/Å^3 and hole of −0.234 e/Å^3. Refinement of the Flack absolute structure parameter *x* for nootkastatin 2 (**5**) with the TWIN/BASF option in SHELXL resulted in a value of 0.00001 with an esd of 0.42445. Attempts at determination of the Flack parameter for the opposite enantiomer of that shown in Figure 3 were thwarted, due to instability in the refinement process. Interestingly, refinement of the opposite enantiomeric structure was possible if the Flack parameter

was excluded as a variable, resulting in an R_1 value of 0.3448 for anisotropic refinement. This is compared with the R_1 value of 0.0744 for the enantiomer shown in Figure 3. These huge differences in *R* values obtained for the two enantiomers produce a dichotomy. On one hand, if the determination of absolute configuration is to be based upon the value of the Flack parameter alone, then the choice of configuration cannot be determined reliably due to the large esd (0.42) observed for the Flack parameter. On the other hand, if assignment of the absolute configuration is determined via application of Hamilton's *R*-factor ratio test,[31] which relies upon the differences in the residual index R_1 values observed for the two possible enantiomers, then a choice can easily be made and unequivocally favors the structure shown in Figure 3. It should be mentioned that the development of the Flack parameter was initiated as an alternative to the older Hamilton *R*-factor ratio test, because of the practical and theoretical difficulties sometimes arising from the use of this older procedure. As a consequence, it is probably advisable to consider the determination of absolute structure for nootkastatin 2 (**5**) as inconclusive because of these inconsistent predictors.

Cancer Cell Line Procedures. Inhibition of human cancer cell growth was assessed using the National Cancer Institute's standard sulforhodamine B assay as previously described.[27] The murine P388 lymphocytic leukemia cell line results were obtained as described previously.[28]

Broth Microdilution Susceptibility Testing of Bacteria. The antibacterial activity of the diterpenes was assessed by the National Committee for Clinical Laboratory Standards (NCCLS) broth microdilution assay.[29] Compounds were reconstituted in a small volume of sterile DMSO and diluted in the appropriate media immediately prior to susceptibility experiments. The MIC was defined as the lowest drug concentration that inhibited all visible growth of the test organism (optically clear). Assays were repeated on separate days. Broth microdilution assays were also performed in media with and without 25% heat-inactivated, filter-sterilized normal human serum (Lampire Biological Labs).

Broth Microdilution Susceptibility Testing of Yeasts. Diterpenes **1**−**5** were screened against yeasts by broth microdilution assays (BMAs) according to the NCCLS.[30] Compounds were reconstituted and MICs defined as above for bacteria.

Minimum Bactericidal and Minimum Fungicidal Concentrations. MBCs and MFCs were determined by subculturing 100 μL from each well with no visible growth in the MIC broth microdilution series onto drug-free plates. The plates were incubated for 24 h (bacteria) or 48 h (yeasts), and the MBC or MFC was defined as the lowest drug concentration that resulted in ≥99.9% reduction in the initial inoculum.

Acknowledgment. We are pleased to thank the following for the very important financial support: Outstanding Investigator Grant CA44344-010-12 and Grant RO1 CA90441-01-03 with the Division of Cancer Treatment and Diagnosis, National Cancer Institute, DHHS; the Arizona Disease Control Research Commission; the Fannie E. Rippel Foundation; the Robert B. Dalton Endowment Fund; Dr. Alec D. Keith; the J. W. Kieckhefer Foundation; the Margaret T. Morris Foundation; Gary L. and Diane R. Tooker; Polly J. Trautman; and Sally Schloegel. We are also pleased to thank the U.S. Forest Service (Tongass National Forest) Supervisor B. Powell, Assistant Supervisor for the Sitkine Division C. Jacobson, Dr. W. Perwick, and C. Schuli (Supervisory Forester), and M. J. Pettit for assisting one of us (G.R.P.) with the field collections. For other very helpful assistance, we thank Profs. C. L. Herald, F. Hogan, and J. M. Schmidt as well as Drs. D. L. Doubek, J. C. Knight, and V. J. R. V. Mukku, and F. Craciunescu, M. Dodson, L. Richert, C. Weber, and L. Williams.

Supporting Information Available: Crystallographic data containing fractional coordinates, isotropic and anisotropic displacement parameters, and bond lengths and angles are available for phenols **2** and **3** and nootkastatin 2. These data may be obtained without charge via the Internet at http://pubs.acs.org.

References and Notes

(1) Contribution 529 of Antineoplastic Agents. For preceding part, see: Pettit, G. R.; Zhang.; Q.; Pinilla, V.; Herald, D. L.; Doubek, D. L.; Duke, J. A. *J. Nat. Prod*., to be submitted.
(2) Pojar, J.; MacKinnon, A. *Plants of the Pacific Northwest Coast*; Lone Pine Publishing: Redmond, WA, 1994; p 41.
(3) (a) Duff, S. R.; Erdtman, H.; Harvey, W. E. *Acta Chem. Scand*. **1954**, *8*, 1073−1082. (b) Erdtman, H.; Harvey, W. E.; Topliss, J. G. *Acta Chem. Scand*. **1956**, *10*, 1381−1392. (c) Erdtman, H.; Topliss, J. G. *Acta Chem. Scand*. **1957**, *11*, 1157−1161.
(4) (a) Zavarin, E.; Anderson, A. B. *J. Org. Chem*. **1956**, *21*, 332−335. (b) Cheng, Y.-S.; Von Rudloff, E. *Phytochemistry* **1970**, *9*, 2517−2527. (c) Cheng, Y.-S.; Von Rudloff, E. *Tetrahedron Lett*. **1970**, *14*, 1131−1132. (d) Norin, T.; Stroemberg, S.; Weber, M. *Chem. Scr*. **1982**, *20*, 49−52.
(5) Johnston, W. H.; Karchesy, J. J.; Constantine, G. H.; Craig, A. M. *Phytother. Res*. **2001**, *15*, 586−588.
(6) Constantine, G. H.; Karchesy, J. J.; Franzblau, S. G.; LaFleur, L. E. *Fitoterapia* **2001**, *72*, 572−574.
(7) Morales-Ramos, J. A.; Rojas, M. G. *J. Econ. Entomol*. **2001**, *94*, 516−523.
(8) (a) Esterfield, T. H.; McDowell, J. C. *Trans. New Zealand Inst*. **1911**, *43*, 55; **1915**, *48*, XXX. (b) Hasegawa, S.; Hirose, Y. *Phytochemistry* **1981**, *20*, 508−510. (c) Cambie, R. C.; Cos, R. E.; Sidwell, D. *Phytochemistry* **1984**, *23*, 333−336. (d) Su, W. C.; Fang, J.; Cheng, Y. *Phytochemistry* **1994**, *35*, 1279−1284. (e) Hanson, J. R. *Terpenoids and Steroids*, *Volume 2, Specialists Periodical Reports*; The Chemical Society, Burlington House: London, 1972; p 130.
(9) Cambie, R. C.; Crump, D. R.; Duve, R. N. *Aust. J. Chem*. **1969**, *22*, 1975−1987. Unfortunately, the original synthetic specimen of phenol **1** was disposed of by the University of Auckland Chemistry Department when Prof. Cambie retired. (G.R.P. wishes to thank Prof. Cambie for that private communication.)
(10) Chow, Y. L.; Erdtman, H. *Acta Chem. Scand*. **1962**, *16*, 1305−1310.
(11) Pettit, G. R.; Gaddamidi, B.; Goswami, A.; Cragg, G. M. *J. Nat. Prod*. **1984**, *47*, 796−801.
(12) Hanari, N.; Yamamoto, H.; Kuroda, K. *J. Wood Sci*. **2002**, *48*, 56−63.
(13) (a) Iwamoto, M.; Ohtsu H.; Tokuda, H.; Matsunaga, S.; Tanaka, R. *Bioorg., Med. Chem*. **2001**, *9*, 1911−1921. (b) Hembree, J. A.; Chang C.; McLauphlin, J. L.; Cassady, J. M.; Watts, D. J.; Wemkert, E.; Fonseca, S.; DePaiva, C. J. *Phytochemistry* **1979**, *18*, 1691−1694.
(14) Kubo, I.; Muroi, H.; Himejima, M. *J. Nat. Prod*. **1992**, *55*, 1436−1440.
(15) Muroi, H.; Kubo, I. *J. Appl. Bacteriol*. **1996**, *80*, 387−394.
(16) Muhammad, I.; Mossa, J. S.; Al-Yahya, M. A.; Ramadan, A. F.; El-Feraly, F. S. *Phytother. Res*. **1995**, *9*, 584−588.
(17) Haraguchi, H.; Oike, S.; Muroi, H.; Kubo, I. *Planta Med*. **1996**, *62*, 122−125.
(18) Nicolson, K.; Evans, G.; O'Toole, P. W. *FEMS Microbiol. Lett*. **1999**, *179*, 233−239.
(19) Evans, G. B.; Furneaux, R. H. *Bioorg. Med. Chem*. **2000**, *8*, 1653−1662.
(20) Evans, G. B.; Furneaux, R. H., Gainsford, G. J.; Murphy, M. P. *Bioorg. Med. Chem*. **2000**, *8*, 1663−1675.
(21) Micol, V.; Mateo, C. R.; Shapiro, S.; Aranda, F. J.; Villalain, J. *Biochim. Biophys. Acta* **2001**, *1511*, 281−290.
(22) Bernabeu, A.; Shapiro, S.; Villalain, J. *Chem. Phys. Lipids* **2002**, *119*, 33−39.
(23) Reid, B. *Discovery*, Quarterly Review of the Royal British Columbia Museum, Autumn 1993.
(24) Bligh, E. G.; Dyer, W. J. *Can. J. Biochem. Phys*. **1959**, *37*, 911−917.
(25) *SAINT+ for NT* v6.04; Bruker AXS, Inc.: Madison, WI, 2001.
(26) *SHELXTL-NT* Version 5.10; Bruker AXS, Inc.: Madison, WI, 1997. An integrated suite of programs for the determination of crystal structures from diffraction data. This package includes, among others, XPREP (an automatic space group determination program), SHELXS (a structure solution program via Patterson or direct methods), and SHELXL (structure refinement software).
(27) Monks, A.; Scudiero, D.; Skehan, P.; Shoemaker, R.; Paul, K.; Vestica, D.; Hose, C.; Langley, J.; Cronise, P.; Vaigro-Wolff, A. *J. Natl. Cancer Inst*. **1991**, *83*, 757−766.
(28) Pettit, G. R.; Meng, Y.; Stevenson, C. A.; Doubek, D. L.; Knight, J. C.; Cichacz, Z.; Pettit, R. K.; Chapuis, J.-C.; Schmidt, J. M. *J. Nat. Prod*. **2003**, *66*, 259−262.
(29) National Committee for Clinical Laboratory Standards 2000. *Methods for Dilution Antimicrobial Susceptibility Tests for Bacteria That Grow Aerobically*, 5th ed.; Approved Standard M7-A5; NCCLS: Wayne, PA, 2000.
(30) National Committee for Clinical Laboratory Standards 1997. *Reference Method for Broth Dilution Antifungal Susceptibility Testing of Yeasts*; Approved Standard M27-A; NCCLS: Wayne, PA, 1997.
(31) Hamilton, W. C. *Acta Crystallogr*. **1965**, *18*, 502−510.

NP0304161